J Solution Chem (2010) 39: 654–664
DOI 10.1007/s10953-010-9537-6

Interaction Between Ranitidine Hydrochloride and Bovine Serum Albumin in Aqueous Solution

Ling-Ling He · Xin Wang · Bin Liu · Jun Wang · Ya-Guang Sun

Received: 9 September 2009 / Accepted: 24 November 2009 / Published online: 12 May 2010

Abstract The interaction between ranitidine hydrochloride (RAN) and bovine serum albumin (BSA) in aqueous solution was investigated by means of fluorescence, synchronous fluorescence, and UV-Vis spectroscopy. The fluorescence of BSA was quenched remarkably by RAN and the quenching mechanism was concluded to be static quenching. The binding constants K and the number of binding sites n were calculated at three different temperatures. The RAN–BSA binding distance was determined to be less than 8 nm, suggesting that energy transfer may occur from BSA to RAN. The interaction process is spontaneous. Based on the obtained thermodynamic parameters, electrostatic forces may play a major role in this process. In addition, the effect of RAN on the conformation of BSA was analyzed using synchronous fluorescence spectra.

Keywords Aqueous solution · Ranitidine hydrochloride · Bovine serum albumin · Interaction

1 Introduction

Ranitidine hydrochloride (RAN, Fig. 1) is N-{2-[[[5-[(dimethylamino)methyl]-2-furanyl] methyl]thio]-ethyl}-N'-methyl-2-nitro-1,1-ethenediamine [1]. It is a histamine H_2-receptor antagonist that has a furan ring structure [2]. It is extensively used in the treatment of active duodenal ulcer, active and benign gastric ulcers, pathogenic gastrointestinal hypersecretory conditions (i.e., Zollinger-Ellison Syndrome), and symptomatic relief of gastroesophageal reflux [3, 4].

L.-L. He · Y.-G. Sun
College of Applied Chemistry, Shenyang Institute of Chemical Technology, Shenyang 110142, P.R. China

X. Wang (✉) · B. Liu · J. Wang
School of Pharmaceutical Sciences, Liaoning University, Shenyang 110036, P.R. China
e-mail: wangxinlnu@yahoo.com.cn

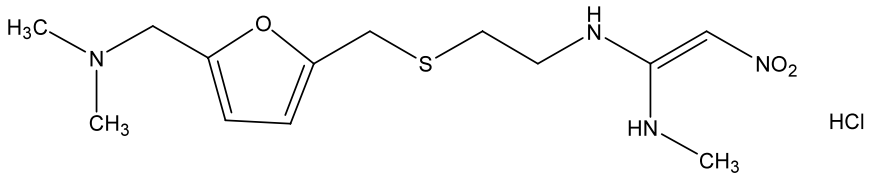

Fig. 1 Molecular structure of RAN

Serum albumin is the most abundant protein in the circulatory system of animals including humans. It is active in the transport of a variety of endogenous and exogenous substances in the body and plays an important role in the distribution and deposition of these substances [5]. Knowledge of interaction mechanisms between drugs and plasma proteins is of crucial importance for understanding the pharmacodynamics and pharmacokinetics of a drug. Drug binding influences the distribution, excretion, metabolism, and interaction with target tissues [6]. Bovine serum albumin (BSA) has been proven to have a high homology and similarity to human serum albumin (HSA) both in sequence and conformation [7]. Therefore, it is always selected as a particularly relevant protein that has become the best-studied model of general drug–protein interactions.

In order to gain some basic information about the interactions of RAN with serum albumin, its in vitro binding with BSA in aqueous solution was investigated by means of various spectroscopic techniques. The binding mechanism between RAN and BSA regarding the binding parameters, the thermodynamic functions, and the effect of RAN on the protein conformation were investigated in this work.

2 Experimental

2.1 Materials

BSA was obtained from Amresco (USA). RAN was obtained from the Liaoning Donggang Hongda Pharmaceutical Co., Ltd. (China). The BSA stock solution, 5.00×10^{-5} mol·L^{-1}, was prepared in a 0.05 mol·L^{-1} Tris–HCl buffer solution of pH = 7.40 containing 0.05 mol·L^{-1} NaCl, then stored at 0–4 °C in a refrigerator. The RAN stock solution, 1.25×10^{-3} mol·L^{-1}, was prepared in the same buffer solution. All of the other materials were of analytical reagent grade and were used without further purification. Doubly distilled water was used to prepare solutions.

2.2 Apparatus and Measurements

All fluorescence measurements were carried out on an LS-55 recording spectrophotometer (Perkin-Elmer, USA) equipped with 1.0 cm quartz cells. The specified temperatures were controlled by air conditioners and a HK-2A digital aqueous thermostat (Nanjing, China). Fluorescence quenching spectra at different temperatures (295, 305 and 315 K) were obtained at an excitation wavelength of 280 nm, with the excitation and emission slit widths set at 2.5 nm. The wavelength interval for synchronous scanning was $\Delta\lambda = 15$ and 60 nm, respectively, at this slit width. The adsorption spectra were recorded on an UV-1201 Spectrophotometer (Beijing, China) with 1.0 cm quartz cells. All pH measurements were made with a pHS-3 digital pH-meter readable to 0.01 pH units (Shanghai, China).

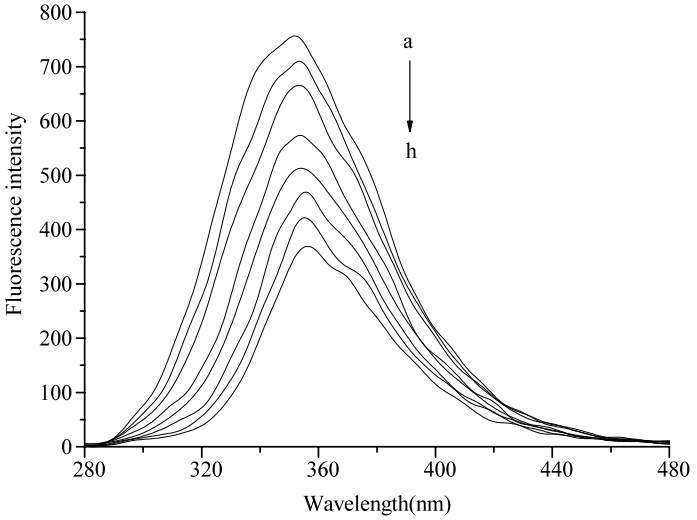

Fig. 2 Fluorescence quenching spectra of BSA in the presence of different concentrations of RAN at 295 K: [BSA] = 1.0×10^{-5} mol·L^{-1}; [RAN] (*a–h*): (0, 0.5, 1.0, 2.0, 3.0, 4.0, 5.0, 6.0) $\times 10^{-5}$ mol·L^{-1}

3 Results and Discussion

3.1 The Fluorescence Quenching Spectra

The fluorescence intensities were corrected for absorption of exciting light and reabsorption of emitted light using the following relationship [8]

$$F_{\text{cor}} = F_{\text{obs}} \times \text{e}^{(A_{\text{ex}}+A_{\text{em}})/2} \tag{1}$$

where F_{cor} and F_{obs} are the fluorescence intensity, corrected and observed, respectively, and A_{ex} and A_{em} are the absorption of the system at excitation and emission wavelength, respectively. The intensity of fluorescence used in this study is always corrected.

Fluorescence quenching refers to any process that decreases the fluorescence intensity of a phosphor. A variety of molecular interactions can result in fluorescence quenching, including excited-state reactions, molecular rearrangements, energy transfer, ground-state complex formation, and collisional quenching [9]. The different mechanisms of fluorescence quenching are usually classified as either dynamic quenching or static quenching. Dynamic quenching and static quenching are caused by diffusion and ground-state complex formation, respectively. They are dependent on temperature to some extent (it is known that higher temperatures result in larger diffusion coefficients), and the dynamic quenching constants are expected to increase with increasing temperature. In contrast, increased temperature is likely to result in decreased stability of complexes, and thus result in lower values of the static quenching constants [10].

In this experiment, BSA is the phosphor while RAN acted as the quencher. The fluorescence spectrum of BSA, and its fluorescence quenching spectra with RAN, were obtained according to literature procedures [11] and are shown in Fig. 2. It is obvious that BSA has a strong fluorescence emission peak at 353 nm after being excited at the wavelength 280 nm. A remarkable decrease of the intrinsic fluorescence of BSA was observed when a fixed concentration of BSA was titrated with different amounts of RAN.

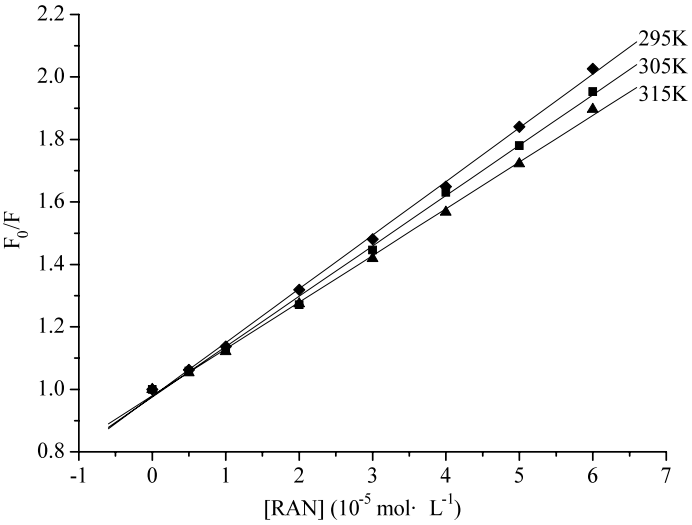

Fig. 3 Stern-Volmer curves of BSA quenched by RAN at different temperatures

3.2 The Fluorescence Quenching Mechanism

In order to confirm the quenching mechanism, we analyzed the fluorescence data at different temperatures with the well-known Stern-Volmer and Lineweaver-Burk equations, which are commonly used in describing dynamic quenching and static quenching, respectively. The Stern-Volmer equation [12, 13] is:

$$\frac{F_0}{F} = 1 + K_q \tau_0 [Q] = 1 + K_{SV}[Q] \tag{2}$$

where F_0 and F represent the fluorescence intensities in the absence and in the presence of quencher, respectively, $[Q]$ is the concentration of the quencher, K_q is the quenching rate constant of the biological macromolecule, K_{SV} is the dynamic quenching constant, τ_0 is the average lifetime of the molecule without any quencher, and the fluorescence lifetime of the biopolymer is 10^{-8} s. The Lineweaver-Burk equation [13, 14] is:

$$(F_0 - F)^{-1} = F_0^{-1} + K_{LB}^{-1} F_0^{-1} [Q]^{-1} \tag{3}$$

where K_{LB} is the static quenching constant with units of $L \cdot mol^{-1}$, which describes the binding efficiency of molecules to biological macromolecules in the ground state.

Fluorescence quenching spectra were measured at three different temperatures and the data have been analyzed with both Eq. 2 and Eq. 3. The curves for these two equations and their correlation coefficients are shown in Figs. 3 and 4, separately. The binding constants and rate constants were calculated and are given in Table 1. The results show that the values of K_{SV} decrease with increasing temperature, which indicates that the quenching mechanism for interaction between RAN and BSA is initiated by complex formation rather than by dynamic collision. The quenching procedure can be further confirmed by the values of K_q. Reference [15] has pointed out that the maximum scatter collision quenching constant of various quenchers with biopolymers is 2.0×10^{10} $L \cdot mol^{-1} \cdot s^{-1}$, and it is obvious that the values of K_q shown in Table 1 are greater than 2.0×10^{10} $L \cdot mol^{-1} \cdot s^{-1}$. Consequently,

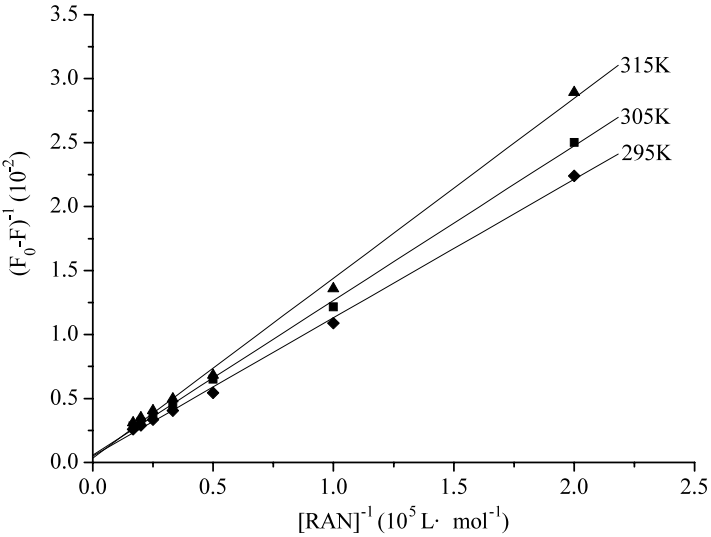

Fig. 4 Lineweaver-Burk curves of BSA quenched by RAN at different temperatures

Table 1 Quenching constants and rate constants of RAN with BSA at different temperatures

T (K)	K_{SV} (L·mol^{-1})	K_q (L·mol^{-1}·s^{-1})	R	K_{LB} (L·mol^{-1})	R
295	1.72×10^4	1.72×10^{12}	0.9993	1.22×10^4	0.9990
305	1.61×10^4	1.61×10^{12}	0.9990	1.15×10^4	0.9994
315	1.50×10^4	1.50×10^{12}	0.9992	1.04×10^4	0.9985

the quenching is static quenching. The values of K_{LB} shown in Table 1 indicate that there is a strong interaction between RAN and BSA. The interaction is weakened as the temperature rises.

3.3 UV-Vis Absorption Spectra

A UV-Vis absorption measurement is a simple but effective method for confirming the probable quenching mechanism. For dynamic quenching, the UV-Vis absorption spectrum of a fluorophore is not changed. Only excited-state fluorescencing molecules are influenced by a quencher. But, for static quenching a compound is formed between the ground state of a fluorophore and quencher; consequently, the absorption spectra of a fluorophore should be influenced [16]. In order to validate the quenching mechanism, the UV-Vis absorption spectra of RAN and BSA were measured (Fig. 5). As seen in Fig. 5, the maximum absorption wavelength of BSA around 280 nm (curve a) shows a red shift and the absorbance intensity obviously increases after addition of an appropriate amount of RAN (curves b–h), which indicates that there is an interaction between RAN and BSA. This result reconfirms that the probable fluorescence quenching mechanism of BSA by RAN is a static quenching process.

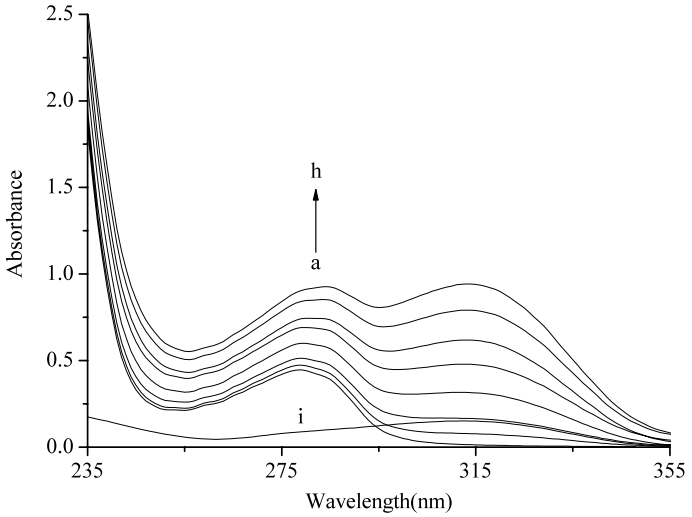

Fig. 5 Absorption spectra of the RAN, BSA and BSA–RAN systems at 295 K. (*a–h*) $[BSA] = 1.0 \times 10^{-5}$ mol·L^{-1}, $[RAN] = (0, 0.5, 1.0, 2.0, 3.0, 4.0, 5.0, 6.0) \times 10^{-5}$ mol·L^{-1}; (i) $[BSA] = 0$, $[RAN] = 1.0 \times 10^{-5}$ mol·L^{-1}

Table 2 The binding constants and the number of the binding sites of RAN with BSA at different temperatures

T (K)	K (L·mol^{-1})	n	R
295	5.88×10^4	1.13	0.9997
305	5.52×10^4	1.13	0.9998
315	5.25×10^4	1.13	0.9997

3.4 Binding Constant and Binding Sites

For a static quenching interaction, if there are similar and independent binding sites in the biomolecule, then the binding constant and the number of binding sites can be gotten from the following double logarithm regression curve [17, 18]:

$$\log_{10}\left(\frac{F_0 - F}{F}\right) = \log_{10} K + n \log_{10}[Q] \tag{4}$$

where K is the binding constant of RAN with BSA and n is the number of binding sites per albumin molecule. Their values can be determined from the slope and intercept of the double logarithm regression cure of $\log_{10}(F_0 - F)/F$ versus $\log_{10}[Q]$ based on Eq. 4. Table 2 gives the resulting values of K and n at different temperatures analyzed in the same way for BSA. The correlation coefficients are between 0.9997 and 0.9998, indicating that the assumptions leading to the derivation of Eq. 4 are satisfactory. The values of n at the experimental temperatures are approximately equal to 1, which indicates the existence of just one single binding site for RAN in BSA.

3.5 Thermodynamic Parameters and Nature of the Binding Forces

Small molecules are bound to macromolecules by four possible binding modes: hydrogen bond, van der Waals, electrostatic, and hydrophobic interactions [19]. In order to clarify the

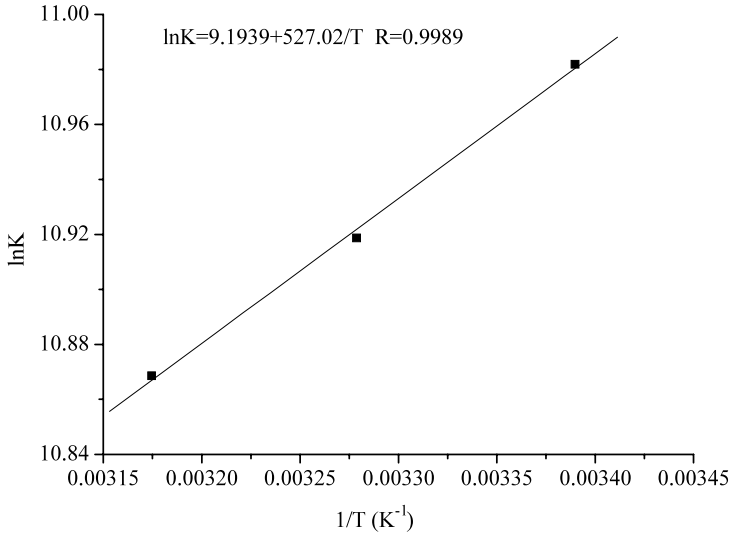

Fig. 6 Van't Hoff plot for the interaction of RAN with BSA

Table 3 Thermodynamic parameters for the interaction of RAN with BSA

T (K)	ΔH (kJ·mol^{-1})	ΔS (J·mol^{-1}·K^{-1})	ΔG (kJ·mol^{-1})
295	−4.38	76.44	−26.93
305			−27.69
315			−28.46

interaction of RAN with BSA, thermodynamic parameters were calculated from Eq. 5 and Eq. 6. If the temperature does not vary significantly, then the enthalpy change (ΔH) can be regarded as a constant. Its value and that of the entropy change (ΔS) can be evaluated from the van't Hoff equation:

$$\ln K = -\frac{\Delta H}{RT} + \frac{\Delta S}{R} \tag{5}$$

where R is the gas constant, T is the experimental temperature, and K is the binding constants at the corresponding T. The data of $\ln K$ versus $1/T$ for the RAN–BSA system are shown in Fig. 6. The enthalpy change (ΔH) and the entropy change (ΔS) were obtained from the slope and intercept of the curve, respectively. Then, the Gibbs energy change (ΔG) can be gotten from the following relationship:

$$\Delta G = -RT \ln K = \Delta H - T\Delta S \tag{6}$$

The thermodynamic parameters for the interaction of RAN with BSA are shown in Table 3. The negative sign for ΔG means that the interaction process is spontaneous. The negative ΔH and positive ΔS values indicate that electrostatic forces may play a major role in the binding between RAN and BSA [20].

3.6 Energy Transfer between RAN and BSA

Fluorescence resonance energy transfer (FRET) has become a "spectroscopic ruler" for measuring molecular distances in biological and macromolecular systems [21]. Generally, FRET occurs whenever the emission spectrum of a fluorophore (donor) overlaps with the absorption spectrum of another molecule (acceptor). The distance between the donor and acceptor and the extent of spectral overlap determine the extent of energy transfer [22]. According to Förster's non-radioactive resonance energy transfer theory [23, 24], the distances between the protein residue and the bound drug in BSA can be calculated by Eq. 7 [25]:

$$E = 1 - \frac{F}{F_0} = \frac{R_0^6}{R_0^6 + r^6} \tag{7}$$

where E denotes the of energy transfer efficiency between the donor and the acceptor, and R_0 is the critical distance where the efficiency of energy transfer is 50%. The value of R_0 can be calculated using the equation:

$$R_0^6 = 8.8 \times 10^{-25} K^2 N^{-4} \Phi_D J \tag{8}$$

where K^2 is the spatial orientation factor related to the geometry of the donor–accepter dipole; $K^2 = 2/3$ for random orientation as in fluid solution; N is the averaged refractive index of the medium in the wavelength range where spectral overlap is significant; Φ_D is the fluorescence quantum yield of the donor; and J is the spectral overlap integral between the fluorescence emission spectrum of the donor and the absorption spectrum of the acceptor. The value of J can be calculated by the following expression:

$$J = \frac{\sum F(\lambda)\varepsilon(\lambda)\lambda^4 \Delta\lambda}{\sum F(\lambda)\Delta\lambda} \tag{9}$$

where $F(\lambda)$ is the corrected fluorescence intensity of the donor in the wavelength range from λ to $\lambda + \Delta\lambda$, and $\varepsilon(\lambda)$ is the molar absorption coefficient of the acceptor when the wavelength is λ.

The overlap of the UV absorption spectrum of RAN with the fluorescence emission spectra of BSA is shown in Fig. 7. In the present case, $N = 1.336$ and $\Phi_D = 0.15$ [26]. From the available data, we can calculate that $J = 5.713 \times 10^{-15}$ cm^3·L·mol^{-1}, $E = 0.1208$, $R_0 = 2.32$ nm, and $r = 3.24$ nm. The binding distance $r = 3.24$ nm is less than 8 nm, and $0.5R_0 < r < 1.5R_0$, which indicates that the energy transfer from BSA to RAN occurs with high probability [27].

3.7 Conformation Investigation

Influences of RAN on the conformational changes of BSA were estimated by synchronous fluorescence measurements. Synchronous fluorescence measurements provide information about the molecular environment in the vicinity of the chromophore molecules and have several advantages: the sensitivity associated with fluorescence is maintained, spectral simplification occurs, spectral bandwidth reduction occurs, and different perturbing effects are avoided [28]. Moreover, the shift of the maximum emission wavelength correlates with changes of the polarity around the chromophores. Synchronous fluorescence spectra were obtained with simultaneously scanning excitation and emission monochromators. As the $\Delta\lambda$

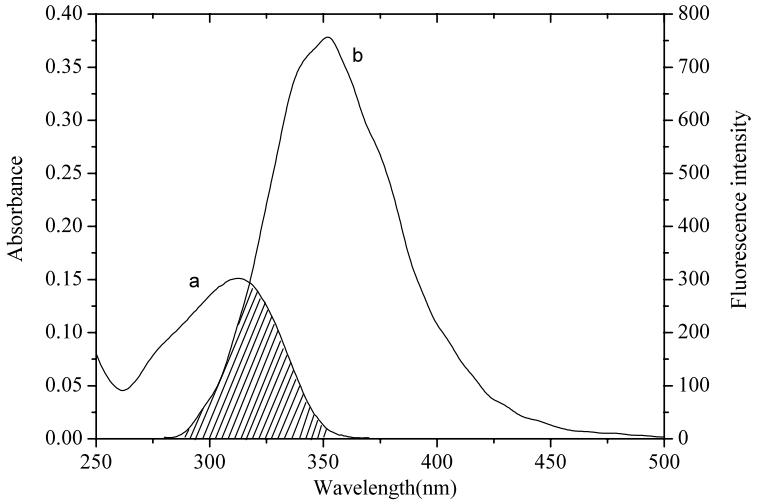

Fig. 7 The overlap of the absorbance spectrum of RAN (*a*) and the fluorescence spectrum of BSA (*b*), where [BSA] : [RAN] = 1 : 1

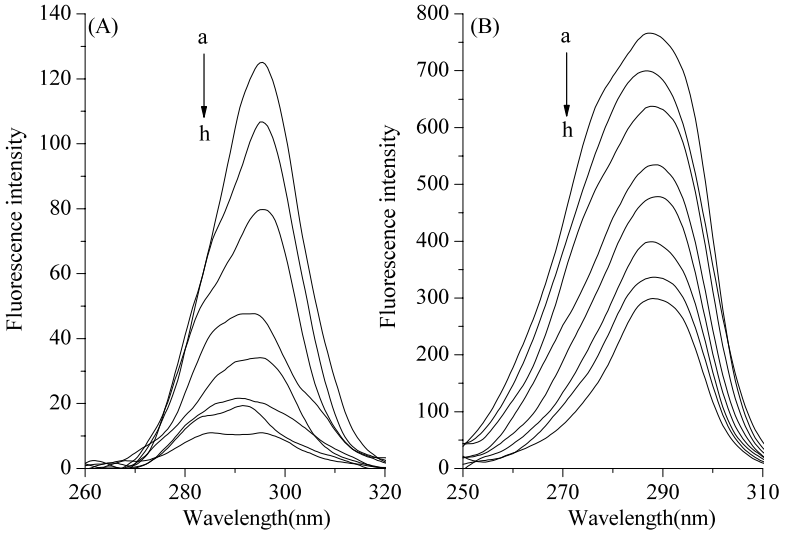

Fig. 8 Synchronous fluorescence spectra of BSA at various concentrations of RAN at $\Delta\lambda = 15$ nm (**A**) and $\Delta\lambda = 60$ nm (**B**). [BSA] $= 1.0 \times 10^{-5}$ mol·L^{-1}; [RAN] (*a–h*): $(0, 0.5, 1.0, 2.0, 3.0, 4.0, 5.0, 6.0) \times 10^{-5}$ mol·L^{-1}

between the excitation wavelength and emission wavelength is 15 nm, synchronous fluorescence offers information about characteristics of the tyrosine residues, while when $\Delta\lambda$ is 60 nm it provides characteristic information about the tryptophan residues [29]. The fluorescence spectra of BSA at various concentrations of RAN for the tyrosine residues and the tryptophan residues are shown in Figs. 8A and 8B, respectively.

In Fig. 8A we observe a gradual decrease of the fluorescence intensity of tyrosine residues and a slight blue shift at the maximum emission upon addition of RAN, which indicates that RAN binds to BSA and is located in close proximity to the tyrosine residues. The conformation of BSA is thus changed, such that the tyrosine residues confront a less polar or more hydrophobic environment [30]. In contrast, in Fig. 8B, only a gradual quenching of fluorescence is observed nearly without any wavelength shift, suggesting that while RAN interacts with tryptophan residues as well, it has hardly any effect on their microenvironment.

4 Conclusions

The interaction between RAN and BSA in aqueous solutions was investigated by means of fluorescence, synchronous fluorescence and UV-Vis spectra. The results show that the probable quenching mechanism of fluorescence of BSA by RAN is a static quenching process, the binding reaction is spontaneous, and is mainly mediated by electrostatic forces. According to Förster's non-radioactive resonance energy transfer theory, energy transfer from BSA to RAN occurs with high probability. The results obtained from synchronous fluorescence spectra show that the structure of BSA molecules is changed remarkably in the presence of RAN. This study is expected to provide important insight into the interactions of serum proteins with RAN.

Acknowledgements This work was supported by the Educational Department Foundation of Liaoning Province, China (No. 2008247).

References

1. Chieng, N., Zujovic, Z., Bowmaker, G., Rades, T., Saville, D.: Effect of milling conditions on the solid-state conversion of ranitidine hydrochloride form 1. Int. J. Pharm. **327**, 36–44 (2006)
2. Kenawi, I.M., Barsoum, B.N., Youssef, M.A.: Drug–drug interaction between diclofenac, cetirizine and ranitidine. J. Pharmaceut. Biomed. **37**, 655–661 (2005)
3. Rivas, J., Gimeno, O., Encinas, A., Beltrán, F.: Ozonation of the pharmaceutical compound ranitidine: reactivity and kinetic aspects. Chemosphere **76**, 651–656 (2009)
4. Lima, L.S., Weinert, P.L., Lemos, S.C., Sequinel, R., Pezza, H.R., Pezza, L.: An environmentally friendly reflectometric method for ranitidine determination in pharmaceuticals and human urine. Spectrochim. Acta A **71**, 1999–2004 (2009)
5. Zhou, N., Liang, Y.-Z., Wang, P.: Characterization of the interaction between furosemide and bovine serum albumin. J. Mol. Struct. **872**, 190–196 (2008)
6. Tang, J.-H., Luan, F., Chen, X.-G.: Binding analysis of glycyrrhetinic acid to human serum albumin: fluorescence spectroscopy, FTIR, and molecular modeling. Bioorgan. Med. Chem. **14**, 3210–3217 (2006)
7. Ghosh, K.S., Sen, S., Sahoo, B.K., Dasgupta, S.: A spectroscopic investigation into the interactions of 3'-*o*-carboxy esters of thymidine with bovine serum albumin. Biopolymers **91**, 737–744 (2009)
8. Anbazhagan, V., Renganathan, R.: Study on the binding of 2,3-diazabicyclo[2.2.2]oct-2-ene with bovine serum albumin by fluorescence spectroscopy. J. Lumin. **128**, 1454–1458 (2008)
9. Zhang, H.-X., Huang, X., Mei, P., Li, K.-H., Yan, C.-N.: Studies on the interaction of tricyclazole with β-cyclodextrin and human serum albumin by spectroscopy. J. Fluoresc. **16**, 287–294 (2006)
10. Zhang, H.-X., Huang, X., Zhang, M.: Thermodynamic studies on the interaction of dioxopromethazine to β-cyclodextrin and bovine serum albumin. J. Fluoresc. **18**, 753–760 (2008)
11. Cao, S.-H., Wang, D.-D., Tan, X.-Y., Chen, J.-W.: Interaction between *trans*-resveratrol and serum albumin in aqueous solution. J. Solution Chem. **38**, 1193–1202 (2009)
12. Xu, H., Liu, Q.-W., Zuo, Y., Bi, Y., Gao, S.-L.: Spectroscopic studies on the interaction of vitamin C with bovine serum albumin. J. Solution Chem. **38**, 15–25 (2009)
13. Zhang, H.-X., Huang, X., Mei, P., Gao, S.: Interaction between glyoxal-bis-(2-hydroxyanil) and bovine serum albumin in solution. J. Solution Chem. **37**, 631–640 (2008)

14. Cheng, Z.-J., Zhang, Y.-T.: Fluorometric investigation on the interaction of oleanolic acid with bovine serum albumin. J. Mol. Struct. **879**, 81–87 (2008)
15. Guo, X.-J., Zhang, L., Sun, X.-D., Han, X.-W., Guo, C., Kang, P.-L.: Spectroscopic studies on the interaction between sodium ozagrel and bovine serum albumin. J. Mol. Struct. **928**, 114–120 (2009)
16. Zhang, G.-W., Wang, A.-P., Jiang, T., Guo, J.-B.: Interaction of the irisflorentin with bovine serum albumin: a fluorescence quenching study. J. Mol. Struct. **891**, 93–97 (2008)
17. Xu, H., Gao, S.-L., Lv, J.-B., Liu, Q.-W., Zuo, Y., Wang, X.: Spectroscopic investigations on the mechanism of interaction of crystal violet with bovine serum albumin. J. Mol. Struct. **919**, 334–338 (2009)
18. Wang, J., Zhang, Y.-Y., Guo, Y., Zhang, L., Xu, R., Xing, Z.-Q., Wang, S.-X., Zhang, X.-D.: Interaction of bovine serum albumin with Acridine Orange (C.I. Basic Orange 14) and its sonodynamic damage under ultrasonic irradiation. Dyes Pigm. **80**, 271–278 (2009)
19. Barbero, N., Barni, E., Barolo, C., Quagliotto, P., Viscardi, G., Napione, L., Pavan, S., Bussolino, F.: A study of the interaction between fluorescein sodium salt and bovine serum albumin by steady-state fluorescence. Dyes Pigm. **80**, 307–313 (2009)
20. Chen, J., Song, G.-W., He, Y., Yan, Q.-J.: Spectroscopic analysis of the interaction between bilirubin and bovine serum albumin. Microchim. Acta **159**, 79–85 (2007)
21. Gharagozlou, M., Boghaei, D.M.: Interaction of water-soluble amino acid Schiff base complexes with bovine serum albumin: fluorescence and circular dichroism studies. Spectrochim. Acta A **71**, 1617–1622 (2008)
22. Zhou, Q.-J., Xiang, J.-F., Tang, Y.-L., Liao, J.-P., Yu, C.-Y., Du, H.-Y., Yang, Q.-F., Xu, G.-Z.: Interaction of spiro [(2R,3R,4S)-4-benzyloxy-2,3-iso-propylidenedioxy-1-oxacyclopentane-5,50-(2-nitromethylene-1,3-diazacyclohexane)] with bovine serum albumin. Pestic. Biochem. Physiol. **92**, 43–47 (2008)
23. Xu, H., Liu, Q.-W., Wen, Y.-Q.: Spectroscopic studies on the interaction between nicotinamide and bovine serum albumin. Spectrochim. Acta A **71**, 984–988 (2008)
24. Zhang, Y.-Z., Zhou, B., Zhang, X.-P., Huang, P., Li, C.-H., Liu, Y.: Interaction of malachite green with bovine serum albumin: determination of the binding mechanism and binding site by spectroscopic methods. J. Hazard. Mater. **163**, 1345–1352 (2009)
25. Wen, M.-G., Zhang, X.-B., Tian, J.-N., Ni, S.-H., Bian, H.-D., Huang, Y.-L., Liang, H.: Binding interaction of xanthoxylin with bovine serum albumin. J. Solution Chem. **38**, 391–401 (2009)
26. Sahoo, B.K., Ghosh, K.S., Dasgupta, S.: Investigating the binding of curcumin derivatives to bovine serum albumin. Biophys. Chem. **132**, 81–88 (2008)
27. Guo, X.-J., Sun, X.-D., Xu, S.-K.: Spectroscopic investigation of the interaction between riboflavin and bovine serum albumin. J. Mol. Struct. **931**, 55–59 (2009)
28. Yue, Y.-Y., Chen, X.-G., Qin, J., Yao, X.-J.: A study of the binding of C.I. Direct Yellow 9 to human serum albumin using optical spectroscopy and molecular modeling. Dyes Pigm. **79**, 176–182 (2008)
29. Wang, C.-X., Yan, F.-F., Zhang, Y.-X., Ye, L.: Spectroscopic investigation of the interaction between rifabutin and bovine serum albumin. J. Photochem. Photobiol. A **192**, 23–28 (2007)
30. Lin, H., Lan, J.-F., Guan, M., Sheng, F.-L., Zhang, H.-X.: Spectroscopic investigation of interaction between mangiferin and bovine serum albumin. Spectrochim. Acta A **73**, 936–941 (2009)